Sustainable Energy, Grids and Networks 26 (2021) 100434

Contents lists available at ScienceDirect

Sustainable Energy, Grids and Networks

journal homepage: www.elsevier.com/locate/segan

Resiliency in active distribution systems via network reconfiguration

Praveen Agrawal [a], Neeraj Kanwar [b,*], Nikhil Gupta [a], K.R. Niazi [a], Anil Swarnkar [a]

[a] Department of Electrical Engineering, Malaviya National Institute of Technology, Jaipur, India
[b] Department of Electrical Engineering, Manipal University Jaipur, India

ARTICLE INFO

Article history:
Received 23 July 2020
Received in revised form 23 September 2020
Accepted 5 January 2021
Available online 9 January 2021

Keywords:
Distributed energy resources
Distribution system
Network reconfiguration
Resiliency
Smart grid

ABSTRACT

Distribution systems have to withstand against natural calamities in such a way that self-healing (SH) persists even during blackout with multiple line faults in the system. Owing to limited power generation from distributed energy resources (DERs), the real challenge behind SH algorithm (SHA) is to restore maximum priority loads (PLs) while satisfying vital network operational constraints besides maintaining better efficiency and reliability of the system. This paper proposes a three-stage SHA to enhance resiliency of distribution systems. Proposed SHA can efficiently restore maximum PLs via network reconfiguration (NR) without intentional islanding during blackout with multiple line faults in the system. The algorithm first transform the faulty distribution network (FDN) into an augmented FDN (AFDN) just to facilitate load flow and tedious mesh checks and then maximizes PLs to be energized while maintaining power balance and other network operational constraints. Finally, AFDN is optimally reconfigured to enhance efficiency and node voltage profile of the system considering uncertain environment of load and generation. Proposed method is demonstrated on a standard test bench while duly addressing a variety of line faults and the results obtained are presented.

1. Introduction

A marked advantage associated with the high penetration of distributed generations (DGs) in distribution systems is that it enhances self-healing (SH) via restoring service to priority loads (PLs) during blackout or/and post fault conditions. SH schemes are an inherent part of the Smart Grid and are expected to play a fundamental role in modern and future distribution systems [1]. Distribution systems are equipped with adequate sensors, communication structures and remote controlled switches (RCSs). This facilitates SH schemes by executing automated network reconfiguration (NR) and load control for optimum operation of distribution systems. Usually, SH is conducted by automatically isolating the faulty section and energizing maximum PLs from DGs till normal supply gets restored. However, the stochastic nature of renewable DG units and load demand, optimal operation and SH of a distribution system are the critical features of future smart grids, but brings new challenges to distribution network operator (DNO) [2]. Such schemes, therefore, should be suitably tailored to improve energy efficiency, power quality and reliability even during acute operating conditions, viz. the occurrence of simultaneous faults during blackout by optimizing self-adequacy in order to stepping ahead towards resilient distribution systems. However, SH schemes need attention towards several issues such as maximization of out-of-service area keeping restoration of highest PLs and energy efficiency whereas minimizing number of switching operations and computational time while satisfying network operational constraints pertaining to node voltage, line currents and radial configuration [3].

SH has been already considered in transmission networks [4–6], but has gained interest from distribution system operators during the last decade. High penetration of DG units in distribution systems has led to evolve this concept by partitioning the distribution system into several interconnected micro grids (MGs) to obtain self-adequacy in SH during a black out or line fault. Self-adequacy refers to generation-load balance within distribution system [2] and that usually cannot be achieved during blackouts. Several important works [2,7,8] have been reported where very useful strategies were proposed for MG-aided service restoration (SR) and optimal operation of the distribution systems, i.e. by sectionalizing the system into multiple MGs [2], employing black-start restoration sequences to ensure system stability, robustness and power quality [7], proposing a multi-criteria decision to exchange power by connecting multiple MGs [8], etc. Whereas, some other works [9–14] have suggested load shedding embedded with NR in order to maximize self-adequacy using DG-powered MGs. The reconfiguration model proposed in [9] builds DG-based islands to restore maximum PLs followed by the occurrence of a fault. A spanning tree method is proposed in [10] to enhance self-healing in distribution systems embedded with microgrids. But, the method does not consider multiple faults. The

* Corresponding author.
E-mail address: nk12.mnit@gmail.com (N. Kanwar).

https://doi.org/10.1016/j.segan.2021.100434
2352-4677/

method suggested in [11] dynamically forms multiple microgrids to restore maximum PLs after the occurrence of multiple faults. The NR scheme of [12] suggests minimization of load shedding considering soft-open points. The load restoration optimization model proposed in [13] coordinates network topology with the formation of microgrids using mixed-integer programming. The contribution of NR to reduce load shedding is nicely reviewed and presented in [14].

From the aforementioned discussion it has been observed that the presence of DGs in reconfigured network provide more reliable, flexible and secured operation via SR and can play crucial role to enhance resiliency of distribution systems under most acute operating conditions. Though SR strategies proposed are interesting and useful but the potential of NR has not been fully exploited using unintentional islanding and does not guarantee the optimality to energize PLs. In addition, most of the works have addressed line fault or black out or both, but natural calamities can never be limited to such simple contingencies. Nevertheless, the SH strategy should be simple, adaptive and must effectively handle even more acute contingencies, e.g. multiple faults during a blackout. Moreover, the stochastic nature of load demand and power generation from renewable DGs, optimal system operation and self-healing in active distribution system, which are the crucial features of future smart grids, have not been duly addressed. However, an increase in information and communication technologies in the electric power system has led distribution systems to a new evolutionary stage known as a smart grid where automatic local switching plans based on an understanding of the network topology and load behaviour allow the implementation of SH strategies [15]. With this philosophy, selected loads can be de-energized using automatic local switching to maximize PLs to be energized, instead employing intentional islanding. The advantage of this strategy is that the network topology remains intact thus avoids operational complexities pertaining to intentional islanding. In addition, the full exploitation of NR to restore maximum PLs can be executed. In fact, SH of power distribution systems is conducted via smart protective and switching devices by automatically isolating faulted components during contingency conditions and then transferring maximum PLs to an optional source when their normal supply has been lost [1]. This could be achieved effectively using automated line and load switches.

With these issues and concerns, this paper proposes a three-stage SH algorithm (SHA) to enhance the resiliency in automated distribution systems (ADSs) during most stringent operating conditions using NR. Proposed SHA first transforms the faulted distribution network (FDN) into an augmented FDN (AFDN) merely to facilitate load flow and mesh checks. The second stage optimizes PLs to be restored thus update AFDN. Finally, the updated AFDN is optimally reconfigured using GA in the third stage to optimize performance of the system while maintaining operational and topological constraints. The novelty of suggested AFDN is that it provides virtual connectivity in the graph of MDN during multiple line faults thus facilitates load flow and mesh checks. This makes SHA highly simplified while dealing with acute operating conditions. First two stages are off-line whereas the third stage is on-line to fully consider uncertainty in load demand and local power generation. The key features of proposed SHA are to

(1) avoid intentional islanding by suggesting AFDN while DN subjected to multiple faults,
(2) maintain power balance while maximizing PLs with no grid supply in FDN,
(3) preserve optimum energy efficiency and node voltage profile while restoring supply,
(4) consider variability in load demand and renewable power generation.

The results of study on a standard test distribution system highlights the importance of proposed method.

2. Proposed self-healing algorithm

Following a natural calamity, grid supply is switched-off whereas the DN may face multiple line faults. While restoring supply, it is desired to achieve good self-adequacy and performance of the system. The limited generation from available resources, unconnected structure of meshed distribution network (MDN) and maintaining operational and topological constraints offer challenging task to SH strategy being devised. The real difficulties arise on account of conducting load flow and tedious mesh checks in an islanded distribution system. Load flow is essential while optimizing PLs to be energized, determining the power generation from the slack bus or reconfiguring DN that also needs tedious mesh checks in the compliance of radiality constraint.

Distribution systems are structured in mesh but can be operated in particular radial topology to achieve desired objectives. For a distribution system with l number of tie-lines, this has been achieved by optimally determining the l number of lines with open status (OS) in the MDN, and the process is known as NR. Optimal NR is to be said as mixed-integer, non-linear and complex combinatorial optimization problem but can be solved efficiently using any population-based metaheuristic technique. These techniques are initialized while keeping in view the graph of MDN. The individuals (tentative solutions) are randomly selected from the graph which are the set of lines having OS, called decision variables (DVs) of the NR problem. These DVs keep on changing in accordance to the control equations or operators of the solution technique. In due course of time, the best individual, having the best functional value, obtained is assumed as the final solution. However, the connectivity of the distribution system must remain intact while employing metaheuristics to solve NR problem. This creates real hurdle while solving NR problem for SH in distribution systems. Another difficulty faced by SH strategy while maximizing PLs as being disbursed among the distribution network. By enlarge, the earlier works reported have proposed SH strategies by sectionalizing distribution system into a cluster of microgrids [2,7–10], but the system operation becomes highly complex while maintaining voltage, current and specifically the power balance constraint on account of dynamically varying states pertaining to stochastic load demand and DG power generation. Moreover, some of the low PLs may remain energized while restoring supply which is a serious concern as then some of the high PLs will not be energized. However, self-healing function as one of the key functions of smart grid brought out as consequence of automation of a smart distribution system [16]. In this context, proposed methodology assumes distribution system with remotely operated line and load switches so that desired distribution line or load may be de-energized/energized in order to maintain desired radial topology and strict restoration of PLs while maintaining optimum performance of the system. Finally, the difficulty arises on account of maintaining power balance with in the distribution network while grid supply is not available. However, the presence of controlled DG unit such as micro-turbine (MT) can resolve the problem if it acts as the slack bus. But, this strategy will be successful unless suitable means are developed to pre-estimate the demand of PLs to be energized, feeder power losses after supply restoration and uncertainty in load demand and power generation from renewable DGs.

However, it will be interesting to have virtual connectivity in the structure of FDN merely to facilitate load flow and mesh checks, but it should not alter electrical properties of the FDN. The network so obtained may be called as AFDN. Therefore, a three-stage SHA is proposed that first determines AFDN being derived from the FDN. AFDN retains virtual connectivity in FDN, but these two networks do not differ electrically. In second stage, optimum PLs are energized by maintaining power balance thus determines tentative power generation from MT. The AFDN with updated load and generation data is then optimally reconfigured in the third stage to enhance the performance of distribution system and also to provide final power generation setting of the MT. First two stages are off-line whereas the third stage is on-line so that the uncertainty in load demand and power generation from renewable DGs can be duly addressed to have more realistic SH solution for the distribution system.

Assuming distribution system to be equipped with RCSs for line as well as load to facilitate desired topology of AFDN using NR and to maximize PLs by switching-off certain loads. The graph of a MDN can be seen as to be composed of different loops as defined by circuit meshes with or without laterals. The junction of two elements is called a node whereas the junction of three or more elements is called principal node. Some vectors are hereby arbitrarily defined for the graph of MDN. The loop branch (*LB*) vector for each loop can be defined as the set of lines which belongs to that particular loop. Some elements of a *LB* vector may belong to only one loop, the set of such circuit elements is called peripheral branch (*PB*) vector, or may belong to two loops, the set of such elements is called common branch (*CB*) vector. In addition, the set of elements of a lateral branch may be called as lateral vector (L_T vector). These vectors fully describe the structure of MDN and are separated by principal node. Each of these vector may face single or multiple line faults during natural calamity. In general, an islanding takes place whenever single fault occur along any L_T vector or at least two line faults occur along the same *PB* or *CB* vector. However, there exists a remote possibility of islanding whenever a particular group of *PB* and *CB* vectors faces a single line fault along each of these vectors called prohibited group vector, a detailed description of which may be referred from [17]. Whatsoever may be the situation, line faults in a DN may be looked as if they have been occurred along $PB/CB/L_T$ vectors. Let us define the set of vectors *L*, *P*, *C* and *LT* which represents the set of *LB*, *PB*, *CB* and L_T vectors, respectively and can be expressed as below:

$$\left.\begin{array}{l} L\colon \{LB(1), LB(2), \ldots, LB(m), LB(n), \ldots\} \\ C\colon \{CB(1,2), CB(2,3), \ldots, CB(m,n), \ldots\} \end{array}\right\} \tag{1a}$$

$$\left.\begin{array}{l} P\colon \{PB(1), PB(2), \ldots, PB(q), \ldots\} \\ LT\colon \{L_T(1), L_T(2), \ldots, L_T(\mathrm{a}), \ldots\} \\ \Omega\colon \{1, 2, \ldots, i, j, \ldots\} \end{array}\right\} \tag{1b}$$

where Ω is the set of all distribution lines. If *i* and *j* represent the lines being in FDN, then following three scenarios of line faults may cover all the variety of line faults.

Scenario A: Single line fault along $PB/CB/L_T$ vector

Scenario B: Any combination of Scenario A

Scenario C: Multiple line faults along $PB/CB/L_T$ vector

Scenario D: Any combination of all the scenarios considered

A detailed description of different scenarios of faults is presented in Table 1. While considering these scenarios, an islanding is not possible in Scenario A or Scenario B unless fault occurs along the L_T vector, but islanding is definite in Scenario C and Scenario D. Whenever islanding takes place, it can be easily tackled while looking the DN along *PB*, *CB* and L_T vectors. The loads being fed from this islanded section can only re-energized if DG(s) of appropriate capacity exists in this section and as such cannot be restored via NR.

Considering a DN with *l* number of tie-lines so the equal number of distribution lines need OS while maintaining radial topology during normal operation. While avoiding intentional islanding, the DN ought to be reconfigured for N-*nc* contingencies including islanding in DN owing to multiple line faults, and with or without grid supply. Therefore, SHA to be devised must address such acute operating conditions of DN that may occur during natural calamity. The real problem arises while dealing with NR problem, as whenever FDN faces islanding the graph of the MDN becomes unconnected which hampers load flow and mesh checks. Besides connectivity of the graph, difficulty arises on account of individual's structure while solving NR problem using metaheuristic technique. These difficulties can be handled tactfully by proposing AFDN and proposed structure of individuals, as explained in the next sub-section.

2.1. Augmented faulty distribution network (AFDN)

In order to facilitate load flow and mesh checks in FDN, determining all the $PB/CB/L_T$ vectors facing line fault(s) thus obtaining fault scenarios. Thereafter, identifying the vector(s) which contributes towards islanding in FDN. In order to retain connectivity of the graph of MDN, following procedure is proposed.

Whenever islanding takes place in a $PB/CB/L_T$ vector, each faulted line within the vector is sequentially substituted by the line with negligible impedance (NI), not with zero impedance line to avoid singularity in Y_{bus} matrix, till the vector transform into a *LT* vector. This vector is called augmented lateral (AL_T) vector. All the loads and generations in the islanded section of AL_T vector is set to zero. In each step of sequential substitution, the connectivity of the graph is judged by determining bus-incidence matrix **A** of the graph of the distribution network so obtained.

Det A will be one or zero for connected or unconnected graph, respectively. The FDN so obtained is called AFDN. The sequential substitution ensures connectivity in the graph of AFDN as it avoids any possibility that the graph remains unconnected. It happened because a remote possibility exists whenever a particular set of AL_T vectors constitutes a cut-set for the graph of MDN, called prohibited group vectors. The detailed explanation about these vectors may be referred from [17]. Since load and generation is set to zero within AL_T vectors and there is no islanding in AFDN, the electrical characteristics of FDN and AFDN remains identical thus load flow and mesh checks can be conducted.

2.2. Individual's structure

Since topological structure of AFDN is quite different than that of MDN, specialized individual's structure is required to solve NR problem using metaheuristic technique. Here, a fact about the AFDN may be stated as, "Each AL_T vector, in general, contains at least one OS line with one or more lines being replaced by NI lines except that AL_T vector which is being transformed from L_T vector of MDN and it contains as many NI lines as there are number of faults, however, these vectors cannot participate while reconfiguring DN". Let,

$'\mathbf{\Omega_{OS}}$: set of *PB* and *CB* vectors with OS lines in the AFDN

$'\mathbf{\Omega_{LT}}$: set of AL_T vectors with NI lines in the AFDN

$\mathbf{\Omega_{OS}}$: set of lines with OS in AFDN of size n_{LOS}

$\mathbf{\Omega_{NI}}$: set of lines with NI in AFDN of size n_{LNI}

Then, the set of lines participating in NR will be given by

$$nc = n_{LOS} + n_{LNI} \tag{2}$$

$\mathbf{\Omega_{LB}}$: set of *LB* vectors with OS or/and NI lines in AFDN of the size n_{LOOP}

$'\mathbf{\Omega_{LB}}$: set of *LB* vectors needs OS lines in AFDN to maintain radial topology of the size n'_{LOOP}

Then,

$$'\Omega_{LB} = L - \Omega_{LB} \tag{3}$$

$$n'_{LOOP} = 1 - n_{LOOP} \tag{4}$$

Table 1
Description of faults in various scenarios.

Scenario	Location of fault	Mathematical representation of fault	Illustration
A	(A1) Along the *PB* of a loop	$i \in PB(p), j \in PB(q); \forall i, j \in \Omega, \forall i = j,$ $\forall PB(p), \forall PB(q) \in P \; \exists \forall p = q$	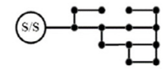
	(A2) Along the *CB* of the loop	$i \in CB(r,s), j \in CB(x,y); \forall i, j \in \Omega, \forall i = j,$ $\forall CB(r,s), \forall CB(x,y) \in C \; \exists \forall r = x \Leftrightarrow \forall s = y$	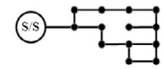
B	(B1) Along the *PB* vectors of different loops	$i \in PB(p), j \in PB(q); \forall i, j \in \Omega, \forall i \neq j,$ $\forall PB(p), \forall PB(q) \in P, \forall p \neq q$	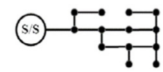
	(B2) Along the *CB* vectors of different loops	$i \in CB(r,s), j \in CB(x,y); \forall i, j \in \Omega,$ $\forall i = j, \forall CB(r,s), \forall CB(x,y) \in C,$ $\exists \forall r \neq x \Leftrightarrow \forall s \neq y$	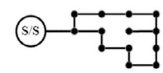
	(B3) Along the *PB* and *CB* vectors of different loops	$i \in PB(p), j \in CB(r,s); \forall i, j \in \Omega, \forall i \neq j,$ $\forall PB(p) \in P, \forall CB(r,s) \in C : \exists \forall PB(p) \subset LB(m)$ $\Leftrightarrow \forall CB(r,s) \cap LB(m) = \{\}, \forall LB(m) \in L$	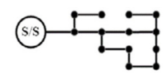
C	(C1) Along the same *PB* vector	$i \in PB(p), j \in PB(q); \forall i, j \in \Omega, \forall i \neq j,$ $\forall PB(p), \forall PB(q) \in P \; \exists \forall p = q$	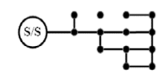
	(C2) Along the same *CB* vector	$i \in CB(r,s), j \in CB(x,y); \forall i, j \in \Omega, \forall i \neq j,$ $\forall CB(r,s), \forall CB(x,y) \in C, \exists \forall r = x \Leftrightarrow \forall s = y$	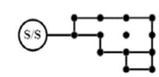
D	Some other combination	A combination of A2 and C2	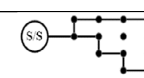

Since all the faulted lines are being replaced by the lines with either OS or NI status in AFDN, therefore individual's structure must contain all lines belongs to $\mathbf{\Omega_{OS}}$ and $\mathbf{\Omega_{NI}}$, and that constitutes a known set of DVs. In addition, the structure must represents (l–n_{LOOP}) number of lines that constitutes unknown set of DVs to be optimized without violating system operational and radial topology constraints. Thus, total lines need OS in reconfigured FDN will be the sum of nc and n'_{LOOP}, *i.e.*

$$N_{OS} = n_{LOS} + n_{LNI} + l - n_{LOOP} \tag{5}$$

However, each DV is selected from one *LB* vector alone where this vector belongs to $'\mathbf{\Omega_{LT}}$. The augmented structure for individuals is, therefore, proposed as shown in Fig. 1. The figure shows that the structure consists of three parts as DVs belongs, directly or indirectly, to different sets $\mathbf{\Omega_{OS}}$, $'\mathbf{\Omega_{LT}}$ and $\mathbf{\Omega_{NI}}$. Since $\mathbf{\Omega_{OS}}$ and $\mathbf{\Omega_{NI}}$ are the known sets of AFDN, the search algorithm has a task to determine only (l–n_{LOOP}) number of DVs from *LB* vectors belongs to $'\mathbf{\Omega_{LT}}$. It is therefore necessary and sufficient that only the middle section of the individual's structure should participate to solve optimal NR problem of AFDN. This reduces dimension of the NR problem. Moreover, these DVs are confined within $'\mathbf{\Omega_{LT}}$. This restricts search space of the problem which consequently improves efficacy and computational burden of the search technique. This immediately implies that more acute the contingency, more will be n'_{LOOP} and consequently more will be the search space reduction. This is noteworthy feature of the proposed method. The augmented structure, however, is used to print the final solution for NR.

$$\underbrace{DV_S \in \Omega_{OS}}_{\text{Length } n_{LOS}} \; \underbrace{DV_S \in LB(m) : \forall mLB(\mathrm{m}) \in {}'\Omega_{LB}}_{\text{Length } n'_{LOOP}} \; \underbrace{DV_S \in \Omega_{NI}}_{\text{Length } n_{LNI}}$$

Fig. 1. Proposed augmented individual's structure.

2.3. An illustration for AFDN

Consider 33-bus test distribution system [18] being modified by the presence of various distributed energy resources (DERs). The MDN of the system without grid supply will be as shown in Fig. 2. Various vectors of MDN are presented in Table 2.

Assuming $\mathbf{\Omega_{FL}}$ as {2, 3, 22, 37}, the FDN will be as shown in Fig. 3. Initially, All faulted lines are assumed with status OS. The figure also shows $\mathbf{\Omega_{LO}}$ and $\mathbf{\Omega_{FV}}$ as {N3, N23, N24 and N25} and {*PB*(1), *CB*(1,2)}, {*PB*(2)}, respectively. While considering $\mathbf{\Omega_{FV}}$, the vector {PB(2)} is facing multiple faults on line 22 and 37. This vector is first augmented by replacing line 22 with NI status. Now all vectors of $\mathbf{\Omega_{FV}}$ are with single fault. For this augmented network, the matrix **A** is evaluated which yet not shows connectivity. This is true as the node N3 yet remained islanded. Therefore any faulted line from the remaining vectors of $\mathbf{\Omega_{FV}}$, i.e. *PB*(1), *CB*(1,2) is replaced by NI status, say line 3 from *CB*(1,2) and again evaluating

Table 2
Various vectors for MDN of 33-bus system.

LB vectors	*LB*(1):{33, 7, 6, 5, 4, 3, 2, 18, 19, 20} *LB*(2): {37, 24, 23, 22, 3, 4, 5, 25, 26, 27, 28} *LB*(3): {35, 11, 10, 9, 8, 33, 21} *LB*(4): {36, 32, 31, 30, 29, 28, 27, 26, 25, 6, 7, 8, 34} *LB*(5): {34, 9, 10, 11, 12, 13, 14}
PB vectors	*PB*(1):{2, 18, 19, 20}, *PB*(2):{22, 23, 24, 37}, *PB*(3):{21, 35} *PB*(4):{15, 16, 17, 36, 32, 31, 30, 29}, *PB*(5):{12, 13, 14}
CB vectors	*CB*(1,2):{3, 4, 5} *CB*(1,3):{33} *CB*(1,4):{6, 7} *CB*(2,4):{25, 26, 27, 28} *CB*(3,4):{8} *CB*(3, 5):{9, 10, 11} *CB*(4,5):{34}
L_T vector	L_T (1):{1}

Table 3
Various sets and parameters obtained for AFDN.

Ω_{OS}	{2, 37}	n_{LOS}	2
Ω_{NI}	{3, 22}	n_{LNI}	2
$'\Omega_{LT}$	{*PB*(2), *CB*(1, 2)}	n_{LOOP}	2
Ω_{LB}	{*LB*(1),{*LB*(2)}	n'_{LOOP}	3
$'\Omega_{LB}$	{*LB*(3), {*LB*(4), *LB*(5)}	N_{OS}	7

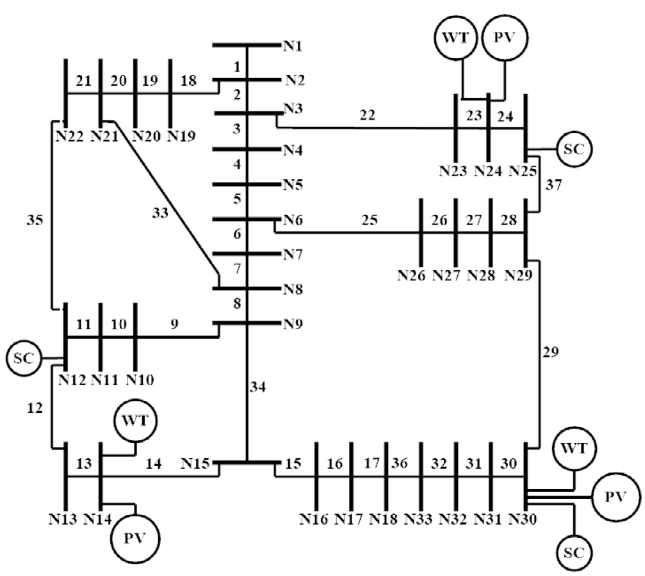

Fig. 2. MDN of the distribution system with grid supply off.

the matrix **A** which shows full connectivity for the augmented network. In this way the vectors *PB*(2) and *CB*(1, 2) becomes AL_T vectors. Now setting zero load on all nodes of $\mathbf{\Omega_{LO}}$ and zero generation on all DERs of $\mathbf{\Omega_{DO}}$ to obtain AFDN as shown in Fig. 4.

Table 3 shows various other sets and parameters obtained for AFDN. The table shows that the length of the augmented individuals' structure N_{OS} is 7 as shown in Fig. 5. The figure shows that DVs are selected from corresponding healthy *LB*s which are quite fewer in number, and not from $\mathbf{\Omega}$, thus significantly reduces problem search space.

2.4. Pre-estimated load demand and reserve for DGs

After obtaining AFDN, the next step is to determine the set of loads which can be restored during contingency period. Owing to limited generation from DG units, loads can be restored on priority basis. Assuming $\mathbf{\Omega_{PL}}$ to be known for the given DN, the

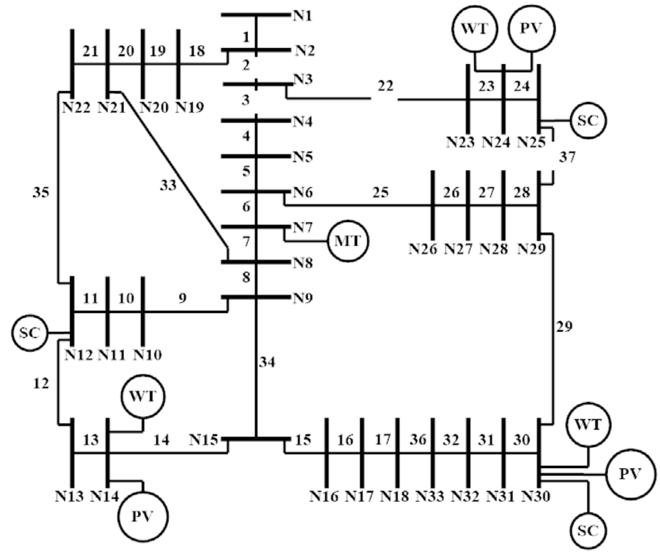

Fig. 3. FDN.

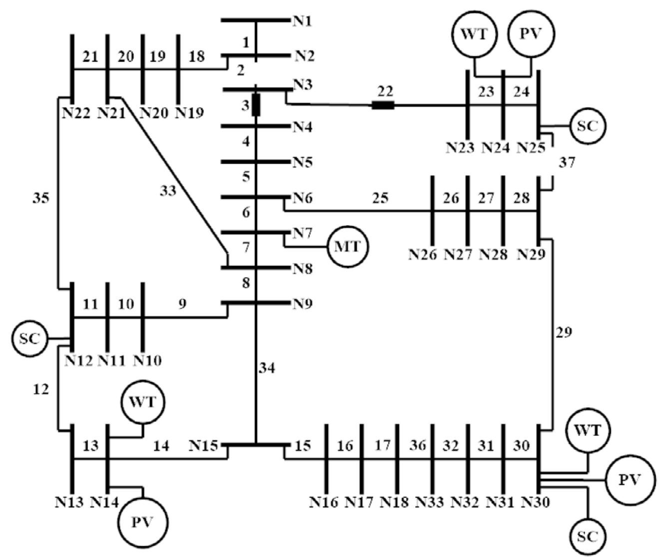

Fig. 4. AFDN.

$$\underbrace{2 \quad 37}_{\text{Length } n_{Los}} \quad \underbrace{DV \in LB(3) \quad DV \in LB(4) \quad DV \in LB(5)}_{\text{Length } n'_{LOOP}} \quad \underbrace{3 \quad 22}_{\text{Length } n_{LNI}}$$

Fig. 5. Augmented individual's structure.

task is to determine $\mathbf{\Omega_{PL,\mathit{st}}}$ the optimum set of PLs to be energized for the given state of the system. Since grid supply is not available, a controlled DG unit, say one MT is selected as the slack bus while conducting load flow. However, the power generation from MT is not possible till the load flow is conducted. It happened because the load flow demands power balance within the DN which requires the exact match of load, feeder power loss and local power generation from all DG units exists in AFDN. But, feeder power loss depends upon the loads constituting $\mathbf{\Omega_{PL,\mathit{st}}}$ and the power generation from MT unit being acting as the slack bus. Therefore, $\mathbf{\Omega_{PL,\mathit{st}}}$ and the power generation from MT is to be determined simultaneously by maintaining power balance within AFDN. Therefore, proposed algorithm is initiated by conducting load flow on AFDN with all loads being energized and measuring power at the slack bus. If the power is found to be more than the rated power of the MT, a load with least priority is curtailed by updating $\boldsymbol{\Omega}_{\mathbf{PL},st}$ and another load flow is conducted. In this way, a sequence of load flows are executed till the slack bus power becomes equal or less than the rated power of the MT. The results of the final load flow simultaneously provides PLs to be energized and the power control of the MT unit. The forecasted data of load and generation from renewable DG is used. However, the proposed strategy may become computationally demanding for large-scale distribution systems. As a remedial measure, the algorithm can be initiated with pre-estimated load demand (PLD), instead of the total load demand on AFDN which can be expressed by the expression (6).

$$P_{D,st}^{pre} \leq \sum P_{PV,k,st}^{fc} + \sum P_{WT,k,st}^{fc} + P_{MT} - P_{L,st} \tag{6}$$

But, feeder power losses are not known while determining PLD, thus imposes difficulty while determining PLD using above mentioned relation. In order to avoid this difficulty, suitable reserve is proposed on the MT unit. The PLD is therefore redefined by the following relation.

$$P_{D,st}^{pre} \leq \sum P_{PV,k,st}^{fc} + \sum P_{WT,k,st}^{fc} + \left(P_{MT} - P_{MT}^{res}\right) - P_{L,st} \tag{7}$$

The reserve considered on MT unit should be sufficient to counter feeder power loss for any radial topology of DN and must be capable to absorb forecasted errors in load and generation from renewable DGs. Therefore, the biggest available MT unit should be selected as the slack bus and the reserve considered should be selected with care, experience and wisdom.

2.5. Network reconfiguration

After obtaining optimum PLs to be energized, the load data of AFDN is updated and then is optimally reconfigured to minimize power losses using real time data of power generation from renewable DGs and load demand. With the system load defines by $\boldsymbol{\Omega}_{\mathbf{PL},st}$ the forecasting errors in load and generation, and the variation in power loss due to NR all needs to be satisfied by the power control of the MT being acting as the slack bus. Therefore, the reserve proposed for the MT unit is set to zero while reconfiguring DN. The power of the slack bus now provides the power scheduling of the MT unit as given by the following relation:

$$P_{MT,st}^{gen,sh} = P_{D,st}^{pre,rt} + P_{L,st}^{rt} - \sum P_{PV,k,st}^{rt} - \sum P_{WT,k,st}^{rt};\ \forall st \in \Omega_{st} \tag{8}$$

The NR problem can be solved using any metaheuristic technique by employing the AFDN shown in Fig. 4. In case the failure duration extends for more than one system state, the DN is optimally reconfigured for each of the concerned state separately. The proposed method thus can be applied to solve NR problem of AFDN while maintain power balance in DN during blackout with multiple line faults in the system. Furthermore, whenever the graph of MDN is found to be broken into two or more connected sub-graphs, the proposed SHA is applied to each of these connected sub-graphs.

With above discussion, a three-stage SHA is proposed to energize maximum PLs during blackout with multiple faults within DN while maintaining power balance and keeping optimum network's efficiency. The FDN is transformed into AFDN in first stage, the second stage maximizes PLs to be energized and then in third stage, AFDN is optimally reconfigured to minimize feeder power losses using genetic algorithm (GA).

GA is preferred over other metaheuristics on account of its simplicity, limited control parameters, and discrete DVs of the problem. And more specifically owing to proposed augmented individual's structure where each DV is constrained by specific *LB* vector, as shown in Fig. 5. The constraint may violate using swarm intelligence based metaheuristics. The flow chart of proposed SHA is shown in Fig. 6.

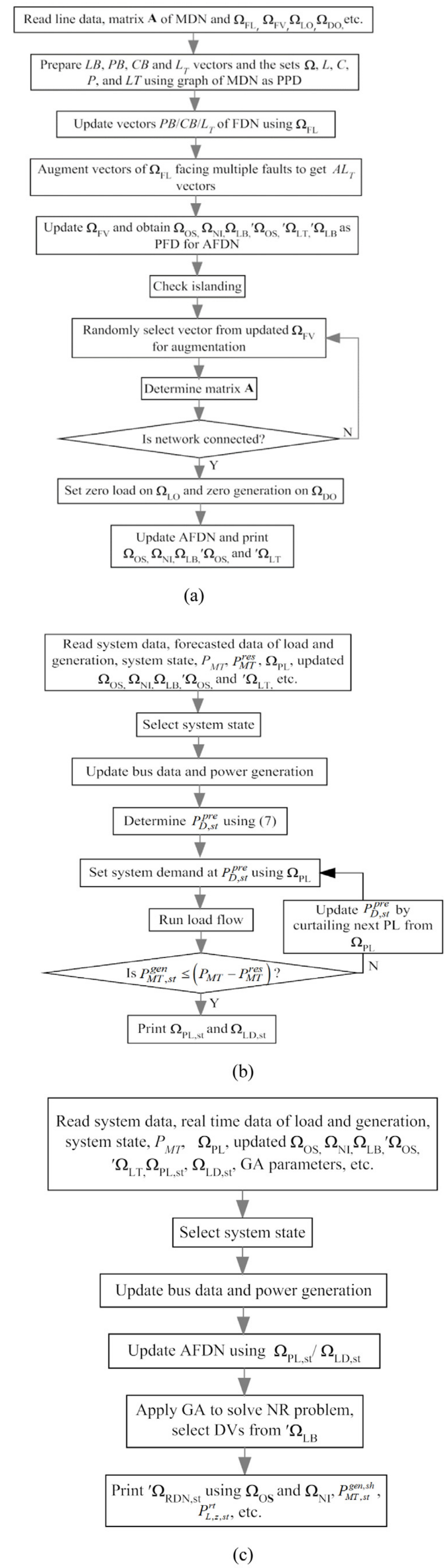

Fig. 6. Flow chart of proposed SHA for (a) Stage I (b) Stage II (c) Stage III.

3. Problem formulation

The SR problem is formulated by considering mix-DER model that includes photo-voltaics (PVs), wind turbines (WTs), MT, and shunt capacitors (SCs) while duly addressing variability and intermittency in load demand and power generation to provide a more realistic scenario for system operation. The aim of the proposed SHA is to determine the most optimal topology for FDN to minimize feeder power losses and maintain node voltage profile, and maximizing PLs during the contingency period while maintaining system operational constraints pertaining to power balance, line currents, node voltages and radial structure of the distribution network. The proposed SHA has three-stages where AFDN is determined in Stage I, PLs are maximized in Stage II and finally AFDN is optimally reconfigured in Stage III. However, the reserve on MT is kept only in Stage II so that it can absorb forecasting errors in load and generation. The first two stages are off-line whereas the third stage is on-line. The problem is formulated for Stage II and Stage III as follows:

Stage II: The objective is to

$$Max\ P_{D,st} = \sum P_{Di\ ,st};\ \forall i \in \Omega_{\mathrm{PL}}, \forall st \in \Omega_{st} \tag{9}$$

where, $P_{Di,st}$ is the load demand of the ith PL, $P_{D,st}$ is the sum of PLs to be remained energized and $\mathbf{\Omega_{PL}}$ is the set of PLs for the state st and $\mathbf{\Omega_{st}}$ is the set of system states.

Eq. (9) is solved using following technical and operational constraints.

$$P_{n+1,st} = P_{n,st} - R_n \frac{P_{n,st}^2 + Q_{n,st}^2}{U_{n,st}^2} - p_{n+1,st};\ \forall n \in \Omega_n, \forall st \in \Omega_{st} \tag{10}$$

$$Q_{n+1,st} = Q_{n,st} - X_n \frac{P_{n,st}^2 + Q_{n,st}^2}{U_{n,st}^2} - q_{n+1,st}; \forall n \in \Omega_n, \forall st \in \Omega_{st} \tag{11}$$

$$U_{n+1,st}^2 = U_{n,st}^2 - 2\left(R_n P_{n,st} + X_n Q_{n,st}\right) + \left(R_n^2 + X_n^2\right) \frac{P_{n,st}^2 + Q_{n,st}^2}{U_{n,st}^2}; \quad \forall n \in \Omega_n, \forall st \in \Omega_{st} \tag{12}$$

$$p_{n+1,st} = p_{n+1,st}^{L} - p_{n+1,st}^{\mathrm{DG}}; \forall n \in \Omega_n,\ \ \forall st \in \Omega_{st} \tag{13}$$

$$q_{n+1,st} = q_{n+1,st}^{L} - q_{n+1,st}^{\mathrm{SC}};\ \ \forall n \in \Omega_n,\ \ \forall st \in \Omega_{st} \tag{14}$$

$$P_{D,st}^{pre} \le \sum P_{PV,k,st}^{fc} + \sum P_{WT,k,st}^{fc} + \left(P_{MT} - P_{MT}^{res}\right) - P_{L,st} \tag{15}$$

$$P_{MT,st}^{gen} = P_{D,st}^{pre} + P_{L,st} - \sum P_{PV,k,st}^{fc} - \sum P_{WT,k,st}^{fc} \tag{16}$$

$$0 \le P_{MT,st}^{gen} \le \left(P_{MT} - P_{MT}^{res}\right) \tag{17}$$

$$P_{TG,st} = \sum P_{PV,k,st}^{fc} + \sum P_{WT,k,st}^{fc} + P_{MT,st}^{gen} \tag{18}$$

$$U_{min} \le U_{n,st} \le U_{max};\ \ \forall n \in \Omega_n,\ \ \forall st \in \Omega_{st} \tag{19}$$

$$I_{n,st} \le I_n^{\max};\ \ \forall n \in \Omega_n,\ \ \forall st \in \Omega_{st} \tag{20}$$

$$nc = n_{LOS} + n_{LNI} \tag{21}$$

$$n'_{LOOP} = l - n_{LOOP} \tag{22}$$

$$N_{OS} = n_{LOS} + n_{LNI} + l - n_{LOOP} \tag{23}$$

$$\Phi_{z,st} = 0 \tag{24}$$

Eqs. (10)–(14) represent the set of general recursive equations to maintain power balance in distribution system. The proposed inequality constraint for pre-estimated load demand is denoted by (15) and the power generation equality and inequality constraints are defined by ((16)–(18)). The node voltage and feeder current constraints are denoted by (19) and (20), respectively. Eqs. (21)–(24) represents network topological constraints to transform given FDN into AFDN. The radial topology constraint is represented by (24) which guarantees zth radial topology of distribution network with no closed path for the state st.

Stage III: The objective is to minimize feeder power loss for the zth radial topology of AFDN which can be expressed as

$$Min\ P_{L,z,st}^{rt} = \sum \frac{R_n\left((P_{n,st}^{rt})^2 + (Q_{n,st}^{rt})^2\right)}{(U_{n,st}^{rt})^2}; \forall n \in \Omega_n, \forall st \in \Omega_{st} \tag{25}$$

Eq. (25) is solved subjected to following constraints:

$$U_{min} \le U_{n,st}^{rt} \le U_{max}; \forall n \in \Omega_n, \forall st \in \Omega_{st} \tag{26}$$

$$I_{n,st}^{rt} \le I_n^{\max}; \forall n \in \Omega_n, \forall st \in \Omega_{st} \tag{27}$$

$$P_{MT,st}^{gen,sh} = P_{D,st}^{pre,rt} + P_{L,st}^{rt} - \sum P_{PV,k,st}^{rt} - \sum P_{WT,k,st}^{rt}; \forall st \in \Omega_{st} \tag{28}$$

$$0 \le P_{MT,st}^{gen,sh} \le P_{MT}; \forall st \in \Omega_{st} \tag{29}$$

$$P_{TG,st}^{rt} = \sum P_{PV,k,st}^{rt} + \sum P_{WT,k,st}^{rt} + P_{MT,st}^{gen,sh} \tag{30}$$

Eqs. (26) and (27) represent node voltage and line current constraints in real time. The scheduled generation from the MT unit considering real time generation from PVs and WTs is for the state st given by (28) which is being constraint by (29) and the total power generation constraint is given by (30). The constraints defined by (10)–(14) are also taken considering real-time data. In addition, topological constraints defined for AFDN using (21)–(24) have also been taken into account. The problem formulation assumed only one MT in the system, but it can be easily extended for several MTs in the system, however, only one of them can be selected as the slack bus.

Table 4
Sizing and siting of DERs.

Node	WT (kW)	PV (kWp)	MT (kW)	SC (kVAr)
N7	–	–	1350	–
N12	–	–	–	300
N14	420	280	–	–
N24	700	840	–	–
N25	–	–	–	300
N30	420	560		600

Table 5
Node voltage and line current limits.

U_{min}/U_{max}(p. u.)	0.94/1.06
$I_{\max}^{n}$(A)/n	400/1, 2; 250/3–5, 18–20, 22–29; 150/6–17, 21, 30–37

4. Simulation results

The proposed method is applied to 33-bus test distribution system [18] which has been extensively preferred for distribution system studies. This is a 12.66 kV radial distribution system with 32 sectionalizing lines (normally closed) and five tie-lines (normally open). The nominal active and reactive load demand for this system are 3.715 MW and 2.30 MVAr. The base configuration of the distribution network obtained by opening the lines 33–37. For this network topology, the feeder power losses are 202.50 kW. The distribution system is modified by assuming the integration of diverse DERs, the sizing and siting of these DERs considered is presented in Table 4. The limits of node voltage and line current have been taken from [19] as shown in Table 5, and the load and generation factors available from the forecasted data are shown in Table 6. The reserve capacity for MT unit is taken as 10%.

The priority of loads considered to constitute Ω_{PL} is presented in Table 7. With no supply from the grid, seven different cases of line faults are considered as shown in Table 8. Proposed method is investigated for these cases while considering system state 19. This system state is specifically considered to simulate a scenario

Table 6
Forecasted load factors and generation factors considered for PVs and WTs.

State	Time (hh:mm:ss)	Load/Generation factor		
		Load	WT	PV
1	00:00:01–01:00:00	0.5421	0.556	0
2	01:00:01–02:00:00	0.5421	0.507	0
3	02:00:01–03:00:00	0.5421	0.484	0
4	03:00:01–04:00:00	0.5421	0.454	0
5	04:00:01–05:00:00	0.5421	0.45	0
6	05:00:01–06:00:00	0.6132	0.49	0
7	06:00:01–07:00:00	0.6829	0.397	0.008
8	07:00:01–08:00:00	0.6829	0.435	0.203
9	08:00:01–09:00:00	0.6829	0.587	0.453
10	09:00:01–10:00:00	0.7421	0.698	0.563
11	10:00:01–11:00:00	0.7421	0.748	0.794
12	11:00:01–12:00:00	0.7421	0.796	0.934
13	12:00:01–13:00:00	0.8711	0.896	0.967
14	13:00:01–14:00:00	0.8000	0.894	0.921
15	14:00:01–15:00:00	0.8711	0.799	0.820
16	15:00:01–16:00:00	0.8711	0.688	0.625
17	16:00:01–17:00:00	0.8711	0.704	0.398
18	17:00:01–18:00:00	0.8711	0.728	0.158
19	18:00:01–19:00:00	0.9303	0.763	0
20	19:00:01–20:00:00	1.0000	0.784	0
21	20:00:01–21:00:00	1.0000	0.806	0
22	21:00:01–22:00:00	0.7513	0.823	0
23	22:00:01–23:00:00	0.5421	0.88	0
24	23:00:01–00:00:00	0.5421	0.911	0

Table 7
Priority of loads.

Priority	Node	Priority	Node	Priority	Node	Priority	Node
1	N24	9	N15	17	N26	25	N33
2	N32	10	N14	18	N28	26	N13
3	N7	11	N29	19	N10	27	N20
4	N31	12	N30	20	N23	28	N8
5	N11	13	N4	21	N22	29	N27
6	N12	14	N17	22	N6	30	N9
7	N3	15	N16	23	N5	31	N19
8	N2	16	N21	24	N18	32	N25

Table 8
Different cases considered for simulations.

Case	Faulted line(s)	Case	Faulted line(s)
1	4	5	2, 3, 22
2	4, 5	6	2, 3, 22, 25
3	9, 10, 11	7	2, 3, 22, 37
4	15, 16, 25	–	–

of fairly good load demand but with acute shortage in the local power generation.

With the distribution network in base configuration, the proposed SHA is first applied to determine AFDN (Stage I) and then PLs to be energized are maximized (Stage II). Thereafter, AFDN is optimally reconfigured for loss minimization (Stage III) using GA algorithm of [17] proposed by the same authors. The population size, maximum generation count, crossover rate and mutation rate for GA are set at 50, 100, 0.95 and 0.05, respectively. The best result obtained after 100 trial runs is presented.

The results obtained for Stage I are summarized in Table A.1 in Appendix. The table also provide self-illustration of the proposed method to obtain AFDN. The knowledge of the sets $\mathbf{\Omega_{LO}}$ and $\mathbf{\Omega_{DO}}$ decides loads and/or DERs to be kept off in the islanded region of DN, if any, before proceeding to stage II. The knowledge of sets $\mathbf{\Omega_{OS}}$, $\mathbf{\Omega_{NI}}$ and variables n_{LOS}, n_{LNI} and n'_{LOOP} provide augmented structure for individuals of GA. Figs. 2–4 may be referred to understand how AFDN is obtained for case-7. Similarly, AFDN for other cases may be obtained. The set $'\mathbf{\Omega_{LB}}$ restricts problem search space of GA while optimally reconfiguring AFDN in Stage III.

The simulation results obtained for stage II are presented in Tables A.2 and A.3 in Appendix. The optimal set of loads to be de-energized, and conversely the optimal set of PLs to be restored is obtained to update AFDN for stage III is presented in Table A.2. The table also shows that SH is above 50% for all the cases considered except in case-7 as some of the DERs are lying in the islanded region. The load flow is conducted over updated AFDN and the results obtained are presented in Table A.3. This off-line result shows local power generations, feeder power loss, and minimum/maximum node voltages considering forecasted data. It is interesting to note that the losses varied widely from 16.07 kW in case-7 to 518.33 kW as in case-6. The small losses are attributed to loss of load and generation in case-7, whereas, NR causes majority of loads to be fed through a long routed feeder thus results in heavy losses in case 6. This is why it is necessary to keep sufficient reserve on the MT unit. The voltage profiles are found within permissible range, except for case-6. It happened because the feeder contains N30 carries about 50% of total system loading and the DERs cause power flow to several downstream nodes as N7 acts as the source bus. As a consequence, the voltage of the tail-end node N24 raised to 1.18 p.u. A capacitor bank at N7 may be helpful to enhance node voltage profile under such acute operating condition. This result has been obtained after relaxing the voltage constraint. The AFDN with the initial configuration shown in the table is reconfigured using GA as per stage III of the SHA and the results obtained are presented in Table 9. It can be observed from the table that the power loss is reduced and node voltage profile is improved using NR. The table also shows the solution vector for NR as per augmented structure of individuals proposed for GA. The solution vector shows bold letters which are the lines with OS being explored using GA while the rest of lines also have OS as they constitute $\mathbf{\Omega_{FL}}$. The fact can be verified using Table A.1. The mean CPU time of GA algorithm is found to be within 13–14 s which is quite reasonable as the total time to restore service usually ranging from 1–5 min [1].

The dynamic reserve available on MT is also presented in the table. DNO can utilize this reserve intelligently and faithfully to energize some additional PLs keeping sufficient reserve to absorb uncertainty in load and generation. Therefore, the decision is subjected to prevailing operating state of the DN. This is how an optimum self-healing can be achieved practically while maintaining operational constraints of the system during acute operating conditions. It has been seen that the distribution system considered can be operated with a self-healing of about 50% without intentional islanding while maintaining better performance under acute conditions of multiple faults with no grid supply and with no power generation from PV units.

5. Conclusions

The paper presents a self-healing algorithm (SHA) using network reconfiguration to restore maximum priority loads without imposing intentional islanding under stringent operating conditions of active distribution systems. Simultaneous multiple faults disrupts connectivity of the graph of distribution system thus imposes challenges to conduct load flow and implementing tedious mesh checks while determining optimal radial topology of faulted distribution network and restoring priority loads. Proposed algorithm efficiently handles these challenges by augmenting the distribution system via virtual connectivity. The novelty of the method lies on the fact that SHA considers original distribution system to be composed of several well-defined smaller sections thus enables the algorithm to be equally valid for any size of distribution system. Simulation results highlights that proposed SHA can simultaneously handle at the most N-(l-1) contingencies. Moreover, the computational efficiency of genetic algorithm improves with the increase in the number of simultaneous faults

Table 9
Simulation results for Stage III.

Case	$'\Omega_{RDN,st}$	$P^{gen,sh}_{MT,st}$ (kW)	$P^{rt}_{TG,st}$ (kW)	$P^{rt}_{L,st}$ (kW)	Min. $U^{rt}_{n,st}$/Max. $U^{rt}_{n,st}$ (p.u.)	$P^{res}_{MT,st}$ (kW)
1	{4, **9**, **13**, **15**, **33**}	819.92	1994.94	120.38	1.00/1.05	530.08
2	{4, **9**, **13**, **15**, **37**, 5}	804.27	1979.29	104.73	1.00/1.05	545.73
3	{9, **33**, **13**, **24**, **15**, 10, 11}	743.64	1918.66	85.97	1.00/1.03	606.36
4	{15, 25, **9**, **12**, **33**, 16}	815.93	1990.95	172.22	1.00/1.06	534.07
5	{2, 22, **14**, **33**, **34**, 3}	847.87	2022.89	148.34	0.99/1.05	502.13
6	{2, 22, 25, **10**, **14**, 3}	1102.48	2277.50	402.95	0.99/1.14	247.52
7	{2, 37, **9**, **32**, **33**, 3, 22}	627.12	1268.04	13.53	0.99/1.01	722.88

thus makes it more suitable for large-scale distribution systems. The restoring of islanded network without controlled local generation is not emphasized, however, can be explored as future extension of the present work. Proposed SHA may also be investigated in the presence of energy storage systems, plug-in electric vehicles while considering cost effectiveness of load switches.

6. Nomenclature

$\boldsymbol{A}$	Bus incidence matrix of meshed distribution network (MDN)
AL_T	Augmented vector with NI line(s) in AFDN
$CB(m, n)$	Common branch vector between mth and nth loop in MDN
$I_{n,st}/I^{rt}_{n,st}$	Current through nth distribution line (off-line)/(real-time) for the state st (p.u.)
$I^n_{\max}$	Current rating of nth distribution line (p.u.)
$LB(m)$	Loop branch vector of the mth *loop* in MDN
L/C/P/LT	Set of loop branch/common branch/peripheral branch/lateral vectors in MDN
L_T(a)	ath lateral vector in MDN
l	Total tie-lines in distribution network (DN)
N_{OS}	Length of the augmented individuals' structure to reconfigure AFDN
Nc	Total contingencies considered for DN
$n_{LOS}/n_{LNI}/n_{LOOP}/n'_{LOOP}$	Size of the set $\Omega_{\rm OS}/\Omega_{\rm NI}/\ \Omega_{\rm LB}/'\Omega_{\rm LB}$
$PB(q)$	Peripheral branch vector for the qth loop in MDN
$P^{pre}_{D,st}/P^{pre,rt}_{D,st}$	Pre-estimated load demand (off-line)/(real-time) for the state st (kW)
$P^{fc}_{PV,k,st}/P^{fc}_{WT,k,st}$	Forecasted generation from kth PV/WT for the state st (p.u.)
P_{MT}	Power rating of MT (p.u.)
$P_{L,st}/P^{rt}_{L,st}$	Feeder power loss (off-line)/(real-time) for the state st (p.u.)
P^{res}_{MT}	Reserve power of MT (p.u.)
$P^{res}_{MT,st}$	Dynamic reserve available on MT during the state st (p.u.)
$P_{Di,st}$	Real power demand of ith load for the state st (p.u.)
$P^{gen}_{MT,st}/P^{gen,sh}_{MT,st}$	MT power generation (off-line)/(real-time scheduling) for the state st (p.u.)
$P^{rt}_{L,z,st}$	Feeder power loss (real-time) for zth radial topology during the state st
$P^{rt}_{n,st}/Q^{rt}_{n,st}$	Real/Reactive power flow (real-time) at nth node for the state st (p.u.)
$P^{rt}_{PV,k,st}/P^{rt}_{WT,k,st}$	Power generation (real-time) from kth PV/WT for the state st (p. u)
$P_{TG,st}/P^{rt}_{TG,st}$	Total power generation from all DGs (off-line)/(real-time) for the state st (p. u)
$P_{n,st}/Q_{n,st}$	Real/reactive power flow (off-line) at nth node for the state st (p.u.)
$p_{n,st}/q_{n,st}$	Injected active /reactive power from DERs (p.u.)
$p^L_{n,st}/q^L_{n,st}$	Real/Reactive power demand of load at nth node for the state st (p.u.)
$p^{DG}_{n,st}$	Active/Reactive power generation at nth node from DG/SC for the state st (p.u.)
R_n/X_n	Resistance/ Reactance of nth distribution line (p.u.)
$S_{H,st}$	Self-healing for the state st
U_{min}/U_{max}	Minimum/Maximum specified node voltage (p.u.)
$U_{n,st}/U^{rt}_{n,st}$	Voltage magnitude at nth node (off-line)/(real-time) for the state st (p.u.)
$\boldsymbol{\Omega}/\boldsymbol{\Omega_n}$	Set of all distribution lines/nodes in MDN
$\boldsymbol{\Omega_{PL}}$	Set of priority loads in DN
$'\boldsymbol{\Omega_{OS}}$	Set of PB and CB vectors with OS lines in AFDN
$'\boldsymbol{\Omega_{LT}}$	Set of AL_T in AFDN
Ω_{OS}/Ω_{NI}	Set of lines with OS/NI in AFDN
$\boldsymbol{\Omega_{LB}}$	Set of LB vectors with OS or/and NI lines in AFDN
$'\boldsymbol{\Omega_{LB}}$	Set of LB vectors needs OS lines in AFDN to maintain radial topology in AFDN
$\boldsymbol{\Omega_{st}}$	Set of system states considered for DN

Table A.1
Simulation results for Stage I.

Particular	Case-1	Case-2	Case-3	Case-4	Case-5	Case-6	Case-7
Ω_{FL}	{4}	{4, 5}	{9, 10, 11}	{15, 16, 25}	{2, 3, 22}	{2, 3, 22, 25}	{2, 3, 22, 37}
Ω_{FV}	{*CB*(1,2)}	{*CB*(1,2)}	{*CB*(3, 5)}	{*PB*(4), *CB*(2, 4)}	{*PB*(1), *CB*(1,2), *PB*(2)}	{*PB*(1), *CB*(1,2), *PB*(2), *CB*(2, 4)}	{*PB*(1), *CB*(1,2), *PB*(2)}
Ω_{LO}	–	{N5}	{N10, N11}	{N16}	{N3}	{N3}	{N3, N23, N24, N25}
Ω_{DO}	–	–	–	–	–	–	{WT2, PV2, SC2}
$'\Omega_{OS}$	{*CB*(1, 2)}	{*CB*(1, 2)}	*CB*(3, 4)}	{*CB*(2, 4)}	{*PB* (1), *CB*(1,2)}	{*PB*(1), *CB*(1,2), *CB*(2,4)}	{*PB*(1), *PB*(2)}
Ω_{OS}	{4}	{4}	{9}	{15, 25}	{2, 3}	{2, 3, 25}	{2, 37}
Ω_{NI}	–	{5}	{10, 11}	{16}	{22}	{22}	{3, 22}
$'\Omega_{LT}$	–	{*CB*(1, 2)}	{*CB*(3,5)}	{*PB*(4)}	{*PB*(2)}	{*PB*(2)}	{*PB*(2), *CB*(1,2)}
Ω_{LB}	{*LB*(1)}	{*LB*(1)}	{*LB*(3), *LB*(5)}	{*LB*(2), *LB*(4)}	{*LB*(1), *LB*(2)}	{*LB*(1),*LB*(2), *LB*(4)}	{*LB*(1), *LB*(2)}
$'\Omega_{LB}$	{*LB*(2), *LB*(3), *LB*(4), *LB*(5)}	{*LB*(2), *LB*(3), *LB*(4), *LB*(5)}	{*LB*(1), *LB*(2), *LB*(4)}	{*LB*(1), *LB*(3), *LB*(5)}	{*LB*(3), *LB*(4), *LB*(5)}	{*LB*(3), *LB*(5)}	{*LB*(3), *LB*(4), *LB*(5)}
n_{LOS}	1	1	1	2	2	3	2
n_{LNI}	0	1	2	1	1	1	2
n_{LOOP}	1	1	1	2	2	3	2
n'_{LOOP}	4	4	4	3	3	2	3
N_{OS}	5	6	7	6	6	6	7

Table A.2
Simulation results for stage II.

Case	$\Omega_{LD,st}$	$\Omega_{PL,st}$	$S_{H,st}$
1	{N5, N6, N8–N10, N13, N18–N23, N25–N28, N33}	{N2–N4, N7, N11, N12, N14–N17, N24, N29–N32}	54.24%
2	{N5, N6, N8–N10, N13, N18–N23, N25–N28, N33}	{N2–N4, N7, N11, N12, N14–N17, N24, N29–N32}	54.24%
3	{N5, N6, N8–N11, N13, N18–N23, N25–N28, N33}	{N2–N4, N7, N12, N14–N17, N24, N29–N32}	53.03%
4	{N5, N6, N8–N10, N13, N16, N18–N23, N25–N28, N33}	{N2–N4, N7, N11, N12, N14, N15, N17, N24, N29–N32}	52.62%
5	{N3, N5, N6, N8–N10, N13, N18–N20, N22, N23, N25–N28, N33}	{N2, N4, N7, N11, N12, N14–N17, N21, N24, N29–N32}	54.24%
6	{N3, N5, N6, N8–N10, N13, N18–N20, N22, N23, N25–N28, N33}	{N2, N4, N7, N11, N12, N14–N17, N21, N24, N29–N32}	54.24%
7	{N3, N5, N6, N8–N10, N13, N16–N28, N33}	{N2, N4, N7, N11, N12, N14, N15, N29–N32}	37.28%

Table A.3
Simulation results for stage II (contd.)

Case	$\Omega_{RDN,st}$	$P^{gen}_{MT,st}$ (kW)	$P_{TG,st}$ (kW)	$P_{L,st}$ (kW)	$Min.U_{n,st}$ (p.u.)	$Max.U_{n,st}$ (p.u.)
1	{4, 33–36}	834.45	2009.47	134.92	1.00	1.04
2	{4, 34–37}	807.61	1982.63	108.08	1.00	1.04
3	{9, 33, 34, 36, 37}	756.79	1931.81	99.12	1.00	1.03
4	{15, 25, 33–35}	820.57	1995.59	176.85	1.00	1.06
5	{2, 22, 34-36}	859.63	2034.65	160.10	0.99	1.05
6	{2, 22, 25, 34, 35}	1217.86	2392.89	518.33	0.99	1.18
7	{2, 34–37}	663.61	1304.53	16.07	0.99	1.01

Ω_{FV}/Ω_{FL}	Set of faulted *PB* and *CB* vectors/faulted lines in DN
Ω_{LO}/Ω_{DO}	Set of loads/DERs in islanded region of DN
$\Omega_{PL,st}/\Omega_{LD,st}$	Set of priority loads remains energized/de-energized for the state *st*
$'\Omega_{RDN,st}$	Solution vector to reconfigured AFDN for the state *st*
$\Omega_{RDN,st}$	Network configuration for AFDN before NR for the state *st*
$\phi_{z,st}$	Close loop for *z*th topology for the state *st*

CRediT authorship contribution statement

Praveen Agrawal: Conceptualization Data curation, Formal analysis, Validation, Visualization. **Neeraj Kanwar:** Conceptualization Data curation, Methodology, Validation, Visualization, Writing - original draft, Writing - review & editing. **Nikhil Gupta:** Investigation, Methodology, Resources, Supervision, Writing - original draft, Writing - review & editing. **K.R. Niazi:** Investigation, Resources, Supervision. **Anil Swarnkar:** Software.

Declaration of competing interest

The authors declare that they have no known competing financial interests or personal relationships that could have appeared to influence the work reported in this paper.

Appendix

See Tables A.1–A.3.

References

[1] J.R. Agüero, Applying self-healing schemes to modern power distribution systems, in: 2012 IEEE Power and Energy Society General Meeting, IEEE, San Diego, CA, USA, 2012, pp. 1–4.

[2] Z. Wang, J. Wang, Self-healing resilient distribution systems based on sectionalization into microgrids, IEEE Trans. Power Syst. 30 (6) (2015) 3139–3149.
[3] Y. Kumar, B. Das, J. Sharma, Multiobjective, multi-constraint service restoration of electric power distribution system with priority customers, IEEE Trans. Power Deliv. 23 (1) (2008) 261–270.
[4] S. Sheng, K.K. Li, W.L. Chan, et al., Agent-based self-healing protection system, IEEE Trans. Power Deliv. 21 (2) (2006) 610–618.
[5] K. Seethalekshmi, S.N. Singh, S.C. Srivastava, A synchrophasor assisted frequency and voltage stability based load shedding scheme for self-healing of power system, IEEE Trans. Smart Grid 2 (2) (2011) 221–230.
[6] A. Golshani, W. Sun, K. Sun, Advanced power system partitioning method for fast and reliable restoration: toward a self-healing power grid, IET Gener. Trans. Distrib. 12 (1) (2018) 42–52.
[7] Y. Wang, C. Chen, J. Wang, et al., Research on resilience of power systems under natural disasters-a review, IEEE Trans. Power Syst. 31 (2) (2016) 1604–1613.
[8] F. Shahnia, S. Bourbour, A. Ghosh, Coupling neighboring microgrids for overload management based on dynamic multicriteria decision making, IEEE Trans. Smart Grid 8 (2) (2017) 969–983.
[9] Y. Xiaodan, J. Hongjie, W. Chengshan, et al., Network reconfiguration for distribution system with micro-grids, in: 2009 Int. Conf. on Sustainable Power Generation and Supply, IEEE, Nanjing, China, 2009, pp. 1–4.
[10] J. Li, X.Y. Ma, C.C. Liu, et al., Distribution system restoration with microgrids using spanning tree search, IEEE Trans. Power Syst. 29 (6) (2014) 3021–3029.
[11] C. Chen, J. Wang, F. Qiu, et al., Resilient distribution system by microgrids formation after natural disasters, IEEE Trans. Smart Grid 7 (2) (2016) 958–966.
[12] Q. Qi, J. Wu, L. Zhang, et al., Multi-objective optimization of electrical distribution network operation considering reconfiguration and soft open points, Energy Proc. 103 (2016) 141–146.
[13] T. Ding, Y. Lin, Z. Bie, et al., A resilient microgrid formation strategy for load restoration considering master–slave distributed generators and topology reconfiguration, Appl. Energy 199 (2017) 205–216.
[14] G. Vaskantiras, Y. Shi, Value assessment of distribution network reconfiguration: a Danish case study, Energy Proc. 100 (2016) 336–341.
[15] J.B. Leite, J.R.S. Mantovani, Development of a self-healing strategy with multiagent systems for distribution networks, IEEE Trans. Smart Grid 8 (5) (2017) 2198–2206.
[16] M. Amin, Challenges in reliability, security, efficiency, and resilience of energy infrastructure: toward smart self-healing electric power grid, in: 2008 IEEE Power and Energy Society General Meeting-Conversion and Delivery of Electrical Energy in the 21st Century, Pittsburgh, PA, USA, 2008, 2008.
[17] A. Swarnkar, N. Gupta, K.R. Niazi, A novel codification for meta-heuristic techniques used in distribution network reconfiguration, Electr. Power Syst. Res. 81 (7) (2011) 1619–1626.
[18] M.E. Baran, F. Wu, Network reconfiguration in distribution system for loss reduction and load balancing, IEEE Trans. Power Deliv. 4 (2) (1989) 1401–1407.
[19] N. Gupta, A. Swarnkar, K.R. Niazi, Reconfiguration of distribution systems for real power loss minimization using adaptive particle swarm optimization, Electr. Power Comput. Syst. 39 (4) (2011) 317–330.